# A Strategy to Explore Stable and Metastable Ordered Phases of Block Copolymers

Weiquan Xu,[†] Kai Jiang,[†] Pingwen Zhang,*[,†] and An-Chang Shi*[,‡]

[†]LMAM and School of Mathematical Sciences, Peking University, Beijing 100871, China

[‡]Department of Physics & Astronomy, McMaster University, Hamilton, Ontario Canada L8S 4M1

**ABSTRACT:** Block copolymers with their rich phase behavior and ordering transitions have become a paradigm for the study of structured soft materials. A major challenge in the study of the phase behavior of block copolymers is to obtain different stable and metastable phases of the system. A strategy to discover complex ordered phases of block copolymers within the self-consistent field theory framework is developed by a combination of fast algorithms and novel initialization procedures. This strategy allows the generation of a large number of candidate structures, which can then be used to construct phase diagrams. Application of the strategy is illustrated using *ABC* star triblock copolymers as an example. A large number of candidate structures, including many three-dimensionally ordered phases, of the system are obtained and categorized. A phase diagram is constructed for symmetrically interacting *ABC* star triblock copolymers.
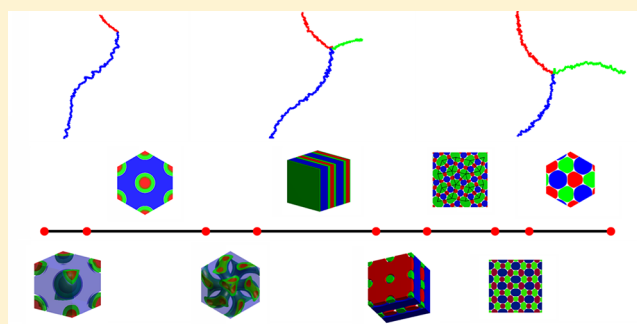
## INTRODUCTION

Block copolymers are macromolecules composed of chemically distinct subchains or blocks. These blocks are covalently linked together to form block copolymers with various topology and architectures. The chemically distinct blocks tend to phase separate, whereas the connectivity of the copolymers prevents a macroscopic separation. The competition of these two opposing trends leads to the formation of various ordered phases.[1,2] The formation of ordered phases of block copolymers and transitions between these phases have been attracting tremendous attention in the past decades. In particular, the self-assembly of block copolymers provides an ideal paradigm for the study of structured soft matter. Furthermore, it has been proposed that the ordered phases of block copolymers possess potentials for applications including lithographic templates for nanowires, photonics crystals, and high-density magnetic storage media.[3]

The self-assembled ordered phases from block copolymers depend sensitively on the chemical compositions, architecture, and topology of the copolymers. The richness of block copolymer phase behavior is exemplified by *AB* diblock copolymers, which are the simplest block copolymers composed of two blocks, *A* and *B*, covalently linked at their ends to form one linear chain. Despite their simplicity, diblock copolymers can self-assemble into various ordered phases, including lamellae (Lam), hexagonally packed cylinders (HCyl), spheres on body-centered cubic or closed-packed lattices (sphere), networked cubic phase (the double-gyroid or gyroid), and orthorhombic phase ($Fddd$ or $O^{70}$).[4] The phase behavior of *AB* diblock copolymers is mainly controlled by the volume fraction of the *A* blocks, $f_A$, and the effective interaction parameter $\chi N$, where $\chi$ is the Flory−Huggins interaction parameter between the different blocks and $N$ is total polymerization of block copolymer. Because of a greatly enlarged parameter space, block copolymers with more complex architectures, such as *ABC* linear or star triblock copolymers, and blends of different block copolymers offer opportunities to create a greater diversity of ordered phases.[5] As an example, recent studies have revealed more than three dozen ordered phases in *ABC* triblock copolymer melts.[6]

Understanding the phase behavior of block copolymers demands a combination of experimental and theoretical approaches. In the past years, a large number of experiments have been carried out to investigate the phase behavior of block copolymers, demonstrating numerous complex ordered phases formed by multiblock copolymers. At the same time, many theoretical and simulation studies have been devoted to the study of block copolymers. These studies have led to a good understanding of the phase behavior of *AB* diblock copolymers. Progress in the understanding of the phase behavior of more complex block copolymers, such as multiblock copolymers with linear and nonlinear architectures, has been slow, largely due to the difficulty in precisely synthesizing different block copolymers experimentally as well as the difficulty in discovering complex ordered phases theoretically.

Because of the flexibility of adjusting system parameters, theory and simulation provide an ideal approach to explore the phase behavior of block copolymers. Theoretically, the major

challenge here is the discovery of different ordered phases, corresponding to local minima of the free-energy functional of the system. This challenge demands the development of accurate free-energy functional for the system and efficient methods to obtain different local minima of the free-energy functional. The current paper presents our continuing efforts to meet this challenge by developing efficient strategies to obtain different local minima of the free energy corresponding to stable and metastable ordered phases of block copolymers. The starting point of our theoretical program is the specification of the free-energy functional for block copolymers. Because of the efforts of a large number of researchers, it has been well-established that the self-consistent field theory (SCFT) of polymers provides a powerful theoretical framework for the study of inhomogeneous polymeric systems in general and the self-assembly behavior of block copolymers in particular.[1,7,8] Our investigation starts with the mean-field free-energy functional within the SCFT framework and aims at the development of strategies to obtain different solutions of the SCFT equations corresponding to possible stable and metastable phases of the system.

Mathematically, the SCFT free-energy functional for a given block copolymer, characterized by its architecture, molecular composition, polydispersity, and block types, is a nonlinear and nonlocal functional of the monomer densities and their conjugate fields.[8] The local minima of the free-energy functional are determined by a set of SCFT equations, which are obtained by minimizing the free-energy functional with respect to the density profiles and fields. The major task in exploring the phase behavior of block copolymers is to find different solutions of the SCFT equations, corresponding to different ordered phases. Because of the complexity of the SCFT equations, efficient numerical methods are required to obtain accurate solutions. The first attempt to solve the SCFT equations numerically was made by Helfand and coworkers.[9] Subsequently, approximate numerical strategies to solve the SCFT equations were developed by Shull[10] and Vavasour and Whitmore[11] to construct phase diagrams of block copolymer melts and solutions. The first accurate numerical solutions of the SCFT equations for diblock copolymers were obtained by Matsen and Schick[12] using a spectral method. Within the spectral method, the spatially varying functions are expanded in terms of a set of basis functions, where the basis functions can be with or without specific symmetries.[12] For ordered structures with known symmetries, the basis functions can be constructed from the given symmetry, leading to accurate and efficient numerical implementations. This powerful method has been extended to investigate the phase behavior of linear ABC triblock copolymer melts[13] and block copolymer blends,[14] leading to the construction of accurate phase diagrams for linear and nonlinear AB-type block copolymers[15,16] and nonfrustrated linear ABC triblock copolymers.[17,18] Later work of Guo et al.[19] has demonstrated that the basis functions can be taken as a generalized Fourier series, allowing them to obtain a number of novel phases for frustrated linear ABC triblock copolymers. Parallel to the development of the spectral-method, numerical techniques to solve the SCFT equations in real space have also been developed, exemplified by Drolet and Fredrickson[20] and Bohbot-Raviv and Wang.[21] Both the real-space method and the generic reciprocal-space method are capable of predicting new ordered phases. An efficient numerical method to solve the SCFT equations combines a split-step method proposed by Rasmussen et al.[22] and a fourth-

order formula proposed by Cochran et al.[23] In what follows, this pseudospectral method to solve the modified diffusion equations will be combined with different initialization strategies to obtain different ordered phases of block copolymers.

The challenge of predicting ordered phases of block copolymers is that, in general, the free-energy functional of a block copolymer system possesses multiple minima, corresponding to various ordered phases that the systems can form. Discovering ordered phases from first-principles requires a method to explore these minima of the free-energy landscape. Because there are no generic methods to find *all* of the minima of a functional, the best strategy is to find as many minima as possible. From this perspective, we propose a two-step strategy to explore the phase behavior of block copolymers. In the first step, fast numerical methods and initialization schemes are combined to obtain as many solutions of the SCFT equations as possible, leading to a library of candidate structures. In the second step, these candidates structures are used as input to more accurate methods to compute their free energies. Finally, a comparison of the free energy of the candidate structures is used to construct phase diagrams of the system. Although the strategy is developed within the SCFT framework from block copolymers, the methodology is applicable to any physiochemical systems exhibiting transitions between different stable and metastable states.

Numerically solutions of the SCFT equations are obtained using iterative techniques. Because of the iterative nature of the algorithms, the solutions crucially depend on the initial configuration at the start of the iteration. In the past years, a variety of initialization procedures have been proposed, including using known ordered phases and random configurations in real and reciprocal space. To obtain as many solutions as possible, we have utilized a variety of initialization procedures in the first step of our calculations. Specifically, initial conditions are generated using (1) knowledge from previous experiments and theories; (2) knowledge from related systems, for example, diblock copolymers; (3) combination and interpolation of known structures; and (4) random initial configurations. Using these diverse strategies of initialization, a large number of candidate ordered phases can be generated as solutions of the SCFT equations. With the increased complexity of block copolymer architectures, the number of candidate phases increases drastically, thus demanding efficient and accurate algorithms. In our study, we used the pseudospectral method in combination with adaptive unit cells to solve the SCFT equations. In the current paper, we will demonstrate the power of the proposed strategy by applying it to the phase behavior of *ABC* star triblock copolymers.

Before we describe the theoretical investigation of *ABC* star triblock copolymers, it is appropriate to briefly summarized the current knowledge of the system. Because of their rich phase behavior, a large number of experimental and theoretical studies have been carried out on the phases and phase transitions of *ABC* star triblock copolymers in the past decades. It has been recognized by Okamoto et al.[24] and Sioula et al.[25] that the *ABC* miktoarm star terpolymers represent a significant block copolymer architecture with a junction point joining three chemically different blocks. The topology of the *ABC* star block copolymers generally confines the junction points to 1D curves as opposed to 2D surfaces, thus resulting in unique self-assembled morphologies. Subsequently, Abetz and coworkers have conducted some interesting experiments investigating the

phase behavior of star triblock copolymers.[26] Furthermore, Matsushita and coworkers have carried out extensive experimental studies on (polyisoprene−polystyrene−poly(2-vinylpyridine)) (ISP) star triblock copolymers, and they have observed numerous ordered tiling patterns (2D ordered phases).[27−31] Besides these two-dimensionally ordered phases, a number of three-dimensionally ordered phases, termed hierarchical structures due to the existence of more than one length scale, have been obtained.[32−34] The phase behavior of ABC star triblock copolymers has also been investigated by computer simulations, leading to valuable insight into their self-assembled structures. Gemma and coworkers[35] performed Monte Carlo (MC) simulations on ABC star triblock copolymers with equal interaction parameters and obtained several tiling patterns. Huang et al. used dissipative particle dynamics simulations to investigate the effects of molecular parameters on self-assembly behavior.[36] Several efforts have also been made to construct phase diagrams of ABC star triblock copolymers using SCFT.[37−39] The stability of the different lamellar morphologies formed from ABC star triblock copolymers has been examined by Xu et al.[40] Most of these previous studies focus on the two-dimensionally ordered phases formed from triblock copolymers near the center of their triangular phase diagram, where the three arms are of equal length. A comprehensive understanding of the self-assembly behavior of ABC star triblock copolymers demands the extension of the calculations to three dimensions and the inclusion of more complex ordered phases. Therefore, the phase behavior of ABC triblock copolymers presents an ideal testing case of the proposed strategy for the discovery of complex ordered phases.

The organization of the article is as follows. The theoretical framework and method of solution are outlined in the SCFT Model and Numerical Algorithms section, using ABC star triblock copolymers as an example. The following Phases and Phase Diagram of ABC Star Triblock Copolymers section is devoted to the presentation and categorization of the obtained candidate ordered phases, including Lamellae-based structures, cylinder-based structures, sphere and gyroid based structures, helix-based structures, combination of basic structures, and 2D structures. A phase diagram for the symmetrically interacting ABC star triblock copolymers is also given in this section, which extends the phase diagram constructed by Zhang et al.[39] by including a number of 3D phases. The final Conclusion and Discussion section presents a brief summary and some outlook on future applications of the strategy as well as a discussion on the utilization of random initialization.

## ■ SCFT MODEL AND NUMERICAL ALGORITHMS

We will use an ABC star triblock copolymer melt as a model system to present the SCFT equations and numerical methods. Generalization to other block copolymers is straightforward. Because there is an extensive literature on SCFT of polymers, only a brief outline of the theory will be given.[8,41] Specifically we consider an incompressible melt of flexible ABC star triblock copolymers with a degree of polymerization $N$ in a volume $V$. The chain lengths of the A, B, and C blocks are $f_A N$, $f_B N$, and $f_C N$ ($f_A + f_B + f_C = 1$), respectively. A characteristic length of the copolymer chain can be defined by $R_0 = \sqrt{N}b$, which is used as the unit of length, so that all spatial lengths are presented in units of $R_0$. Within the mean-field approximation to the many-chain system at a temperature $T$,[8,41] the free-

energy functional $F$ per chain of the triblock copolymer melt is given by

$$\frac{F}{nk_BT} = -\ln Q + \frac{1}{V}\int d\mathbf{r}\Big\{\sum_{\alpha\neq\beta}\chi_{\alpha\beta}N\phi_\alpha(\mathbf{r})\phi_\beta(\mathbf{r}) \\ - \sum_\alpha \omega_\alpha(\mathbf{r})\phi_\alpha(\mathbf{r}) - \eta(\mathbf{r})[1 - \sum_\alpha \phi_\alpha(\mathbf{r})]\Big\} \tag{1}$$

where $\alpha,\beta \in \{A, B, C\}$ are the block labels, $\phi_\alpha$ is the local concentration of the $\alpha$-blocks, and $Q$ is the partition function of one star block copolymer chain in the mean field, $\omega_\alpha$, which in turn are produced by the surrounding chains. The interactions between the three chemically distinct monomers are characterized by three Flory−Huggins interaction parameters $\chi_{BC}$, $\chi_{AC}$, and $\chi_{AB}$. Minimization of the free-energy functional with respect to the monomer densities and the mean fields subjected to the incompressible condition leads to the following set of mean-field equations or SCFT equations[41]

$$\omega_A(\mathbf{r}) = \chi_{AB}N\phi_B(\mathbf{r}) + \chi_{AC}N\phi_C(\mathbf{r}) + \eta(\mathbf{r})$$

$$\omega_B(\mathbf{r}) = \chi_{AB}N\phi_A(\mathbf{r}) + \chi_{BC}N\phi_C(\mathbf{r}) + \eta(\mathbf{r})$$

$$\omega_C(\mathbf{r}) = \chi_{AC}N\phi_A(\mathbf{r}) + \chi_{BC}N\phi_B(\mathbf{r}) + \eta(\mathbf{r})$$

$$\phi_A(\mathbf{r}) = \frac{1}{Q}\int_0^{f_A} ds\, q_A(\mathbf{r}, s)q_A^+(\mathbf{r}, 1 - s)$$

$$\phi_B(\mathbf{r}) = \frac{1}{Q}\int_0^{f_B} ds\, q_B(\mathbf{r}, s)q_B^+(\mathbf{r}, 1 - s)$$

$$\phi_C(\mathbf{r}) = \frac{1}{Q}\int_0^{f_C} ds\, q_C(\mathbf{r}, s)q_C^+(\mathbf{r}, 1 - s)$$

$$Q = \frac{1}{V}\int d\mathbf{r}\, q_K(\mathbf{r}, s)q_K^+(\mathbf{r}, 1 - s)$$

$$1 = \phi_A(\mathbf{r}) + \phi_B(\mathbf{r}) + \phi_C(\mathbf{r}). \tag{2}$$

In these expressions, the functions $q_K(\mathbf{r},s)$ and $q_K^+(\mathbf{r},s)$ ($K \in \{A, B, C\}$) are the end-integrated segment distribution functions, or propagators, representing the probability of finding the $s$th segment at a particular position $\mathbf{r}$. These propagators satisfy the modified diffusion equations[41]

$$\frac{\partial q_K(\mathbf{r}, s)}{\partial s} = \frac{1}{6}\nabla_\mathbf{r}^2 q_K(\mathbf{r}, s) - \omega_K(\mathbf{r}, s)q_K(\mathbf{r}, s),$$

$$q_K(\mathbf{r}, 0) = 1;$$

$$\frac{\partial q_K^+(\mathbf{r}, s)}{\partial s} = \frac{1}{6}\nabla_\mathbf{r}^2 q_K^+(\mathbf{r}, s) - \omega_K(\mathbf{r}, s)q_K^+(\mathbf{r}, s),$$

$$q_K^+(\mathbf{r}, 0) = q_L(\mathbf{r}, f_L)q_M(\mathbf{r}, f_M), \tag{3}$$

where $(KLM) \in \{(ABC), (BCA), (CAB)\}$. Numerically solving these SCFT equations involves an iterative procedure starting with an initial guess of the fields $\omega_K(\mathbf{r})$ (with $K \in \{A, B, C\}$). The modified diffusion equations (eq 3) are then solved to obtain the propagators, which are used to compute the densities $\phi_K(\mathbf{r})$ and then to update the mean fields $\omega_K(\mathbf{r})$. The iteration is continued until these mean fields and densities are self-consistent such that they satisfy the SCFT equations (eq 2) within a prescribed numeric accuracy.

The search of candidate phases requires efficient and accurate algorithms to solve the modified diffusion equations eq 3. In
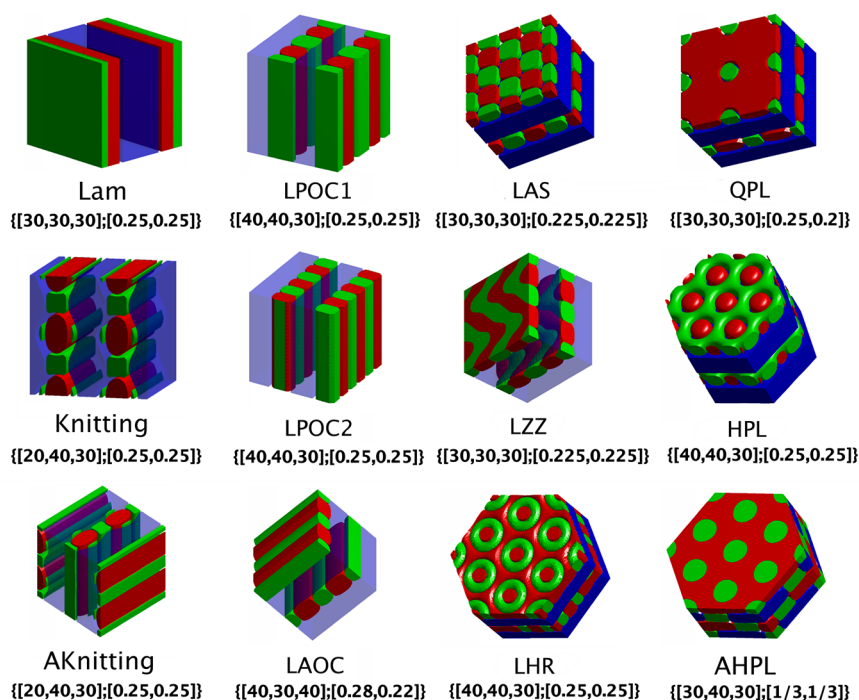
**Figure 1.** Lamellae-based structures obtained in our simulation. Monomers *A*, *B*, and *C* are denoted by red, green, and blue colors. Parameters used here are denoted as $\{[\chi_{BC}N, \chi_{AC}N, \chi_{AB}N];[f_A, f_B]\}$ below figures of each microphase. Except in AHPL, *C* monomers in all of these structures form lamellae structure while *A* and *B* monomers form substructure between *C* layers. In AHPL, *A* and *C* monomers form a similar but translated hexagonal perforate lamellae with *B* monomer filling the cavity.

this work, we have used the improved pseudospectral method with a fourth-order accuracy as proposed by Rasmussen et al.[22] and by Cochran et al.[23] The pseudospectral method requires transitioning between real and reciprocal spaces. We expand all spatial functions in terms of plane waves. The number of plane-wave basis functions is 32 × 32 × 32, so there are 32 plane waves along the *x*, *y*, and *z* directions. In general, unit cells with arbitrary shape and size can be used to generate the basis functions. In practice, we use a cubic unit cell in most of our calculations. It should be noticed that many ordered phases, such as the 2D morphologies, hexagonally perforated lamellae, and *Fddd*-type structures, require noncubic unit cells. The basis functions with a cubic unit cell are plane waves of the form $\exp[2\pi i(lx + my + nz)/D]$, where *D* is the size of the cubic cell and $l,m,n \in [-16,15]$. The size of the unit cell *D* is a variable that is determined by the minimization of the free energy. The propagators, $q_K(\mathbf{r},s), q_K^+(\mathbf{r},s)$; $s \in [0, f_K]$, are functions of the space and the contour length *s*. While the spatial variable is discretized using the Fourier expansion, the contour length *s* in the interval $[0, f_K]$ is discretized into $N_K$ substeps. To ensure the accuracy, we require that these substeps are smaller than a prescribed tolerance $f_K/N_K \leq \varepsilon$ with $\varepsilon = 0.01$.

In our computations, we have utilized several strategies to set up the initial mean fields, $\omega_K(\mathbf{r})$ $(K \in \{A, B, C\})$, which could lead to solutions with different symmetries. First of all, well-known block copolymer systems such as the diblock copolymers provide knowledge about the symmetry of ordered block copolymer phases, which can be used as guidance to set up initial mean fields. Second, available experimental data, such as the scattering patterns, provide important input for the setup of the initial mean-fields. Finally, the symmetry of ordered phases can be "designed" by introducing predetermined density profiles. For example, the combination of lamellae and cylinders can be used to produce two possible ordered phases, the layers of parallel oriented cylinders (LPOCs) and the layers of alternatively oriented cylinders (LAOCs), as shown in Figure 1. Another example is the Knitting pattern shown in Figure 1, which can be considered as a variation of the LPOC phase. The analogous alternative version of the Knitting Pattern, the AKnitting phase, can then be obtained naturally via interpolation of the LAOC phase. One way to summarize the strategies for the discovery of complex ordered phases is that complex ordered phases can be constructed from simpler phases that are obtained from existing experimental, simulations, and theoretical data. These structures can then be used as initial density profiles. Once converged, the different solutions from the various initial configurations can lead to different ordered phases as solutions of the SCFT equations.

## PHASES AND PHASE DIAGRAM OF *ABC* STAR TRIBLOCK COPOLYMERS

For a generic block copolymer melt, the phase behavior is controlled by a number of parameters including the volume fractions, $f_\alpha$, of the blocks, the Flory–Huggins interaction parameters, $\chi_{\alpha\beta}$, and the Kuhn lengths of the different monomers. For a given set of these parameters, the SCFT equations can have a number of solutions, corresponding to the stable and metastable phases of the system. We will first enumerate a large number of candidate structures obtained from our extensive SCFT computations. All of these structures are solutions of the SCFT equations. Therefore, they correspond to local minima of the free-energy landscape of the system, although most of these phases are metastable. These candidate phases are then used to construct phase diagrams. To compare with the theoretical phase diagrams available in the literature,[39] we will focus on the phase diagram
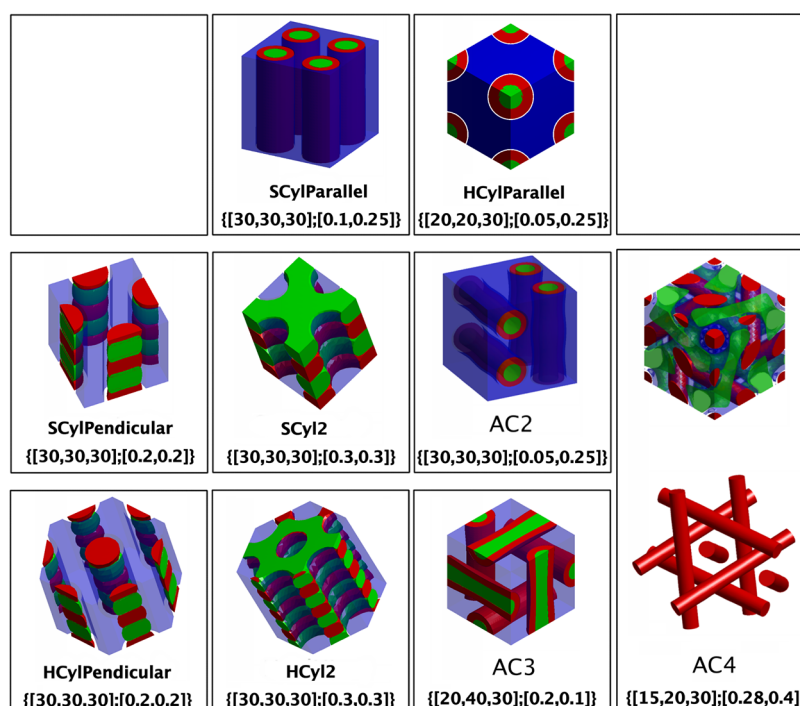
**Figure 2.** Cylinders-based structures with diverse hierarchical phase separation and orientation. Two different types of hierarchical phase separation, inside or outside the cylinders, are shown here. AC2, AC3, and AC4 denote alternative cylinders with two, three, and four different orientations, respectively. As for AC4 enclosed in a rectangle, we add a schematic illustration that is reconstructed from the Fourier coefficients of *A* segment density distribution.

of symmetrically interacting *ABC* star triblock copolymers with fixed Flory–Huggins parameters, $\chi_{BC}N = \chi_{AC}N = \chi_{AB}N = 30$.

**Candidate Structures for *ABC* Star Triblock Copolymers.** Utilizing the different initialization procedures outline above, we have obtained a large number of solutions of the SCFT equations for the *ABC* star triblock copolymers. These candidate phases range from simple variations of the diblock copolymer phases to complex hybridization of the different building domains (lamellae, cylinders, and spheres). These candidate structures are presented in this subsection, which are categorized by their basic overall morphologies.

The concept of basic overall structures of ABC star triblock copolymers is derived from our knowledge of the phase behavior of A–C diblock copolymers, or more precisely, $A_2$-C star triblock copolymers.[4,45,46] As the volume fraction of one of the blocks, for example, $f_C$ of the *C* block, is increased or decreased from 0.5, A–C diblock copolymers self-assemble to form lamellae, gyroids, cylinders, and spheres. For an *ABC* star triblock copolymer, the phase behavior would be similar to the corresponding diblock copolymers if two of the blocks, for example, *A* and *B* blocks, are miscible. In this case, the phase behavior of the *ABC* triblock copolymers is expected to be similar to a corresponding $A_2$–C star triblock copolymer. Therefore, we expect that the overall structure of the system changes from lamellae to gyroids to cylinders and finally to spheres as the volume fraction of the *C* blocks increases from 0.6.[4,45,46] In the cases where the *AB* blocks are immiscible, the *AB* blocks will separate within the lamellae, cylinders, or spheres, leading to the formation of complex phases according to the patterns formed by the *AB* blocks. Furthermore, different packing patterns of the spheres, such as the A-15 structure, can be formed from the $A_2$–C star triblock copolymers.[4,45,46] From this perspective, it is useful to classify these complex phases into

lamella-based phases, cylinder-based phases, sphere-based structures, gyroid-based structures, helix-based structures, as well as combinations of the basic structures and 2D tiling patterns.

*Lamella-Based Structures.* On the basis of understanding the phase behavior of diblock copolymers, we expect that the *ABC* star triblock copolymers, with the volume of one of its blocks being ~50% of the copolymer, for example, $f_C \approx 0.5$, tend to form lamellae composed of alternative *AB* and *C* layers. In particular, the self-assembled phase should be lamellae composed of alternating *C* layers and mixed *AB* layers when the *A* and *B* blocks are miscible ($\chi_{AB} \approx 0$). Increasing the *AB* repulsion will lead to separation of *A* and *B* blocks within the *AB* layers. The different patterns formed by the *A* and *B* blocks lead to a variety of lamella-based complex phases of *ABC* star triblock copolymers. The Lamella-based phases obtained from our SCFT computations are shown in Figure 1. Besides the simple lamellae (Lam) in which the *A* and *B* blocks form disordered *AB* layers, various Lamella-based phases with different patterns of *AB* separations can be formed, leading to a very rich array of complex candidate phases.

The simplest *AB* separation pattern is for the *A* and *B* blocks forming alternating cylinders. These cylinders in different layers can be packed and oriented differently, leading to a number of cylinders-in-layers structures. Specifically, the *AB* cylinders in alternating layers can be parallel or perpendicular to each other, leading to two types of structures, the LPOCs and the LAOCs. Furthermore, the cylinder packing in different layers in the LPOC structure can be the same as displaced, leading to the LPOC1 and LPOC2 phases shown in Figure 1.

More complex *AB* separation patterns lead to the formation of the knitting pattern (Knitting) shown in Figure 1, which can also be viewed as a structure formed from *AB* cylinders. These
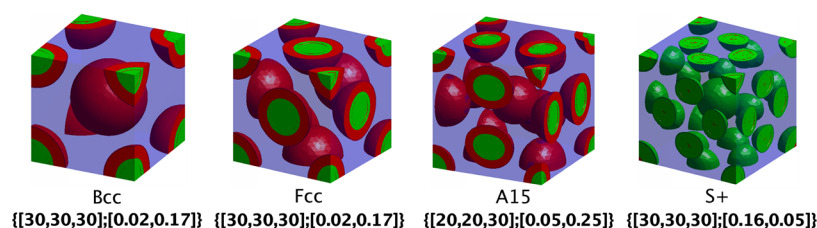
| Bcc | Fcc | A15 | S+ |
|---|---|---|---|
| {[30,30,30];[0.02,0.17]} | {[30,30,30];[0.02,0.17]} | {[20,20,30];[0.05,0.25]} | {[30,30,30];[0.16,0.05]} |

**Figure 3.** Typical spheres-based structures.



| CS–SGyroid | CS–DGyroid | AS–SGyroid | AS–DGyroid |
|---|---|---|---|
| {[20,20,30];[0.05,0.3]} | {[20,20,30];[0.05,0.25]} | {[30,30,30];[0.2,0.2]} | {[30,30,30];[0.2,0.2]} |
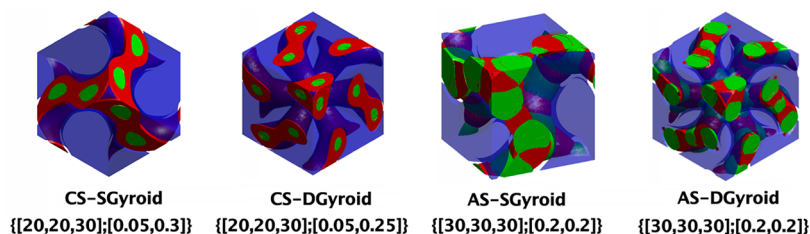
**Figure 4.** Typical gyroid-based phases structures. Both single gyroid (SG) and double gyroid (DG) are shown here, with core−shell and hierarchical version.

*AB* cylinders can orient differently in different layers, forming the alternating knitting pattern (AKnitting) shown in Figure 1. It is interesting to noticed that for the parameters $[\chi_{BC}N, \chi_{AC}N, \chi_{AB}N] = [20, 40, 30]$ and $f_A = f_B = 0.25$, the AKnitting phase has a slightly lower free energy than Knitting pattern. Furthermore, the 2D *AB* separation can be more diverse within the *AB* layers, leading to more complex ordered phases including the layers with alternate spheres (LAS), layers with zigzag cylinders (LZZ), layers with hexagonal rings (LHR), and perforated layers with different arrangement of the pores (QPL and HPL).

Another interesting candidate structure is the alternating hexagonal perforated layered (AHPL) structure, in which the *A* and *C* blocks form hexagonal perforate lamellae with the *B* monomer filling the cavity (Figure 1). Although in AHPL we use $f_A = f_B = f_C = 1/3$ (rather than $f_C \approx 0.5$ for all other structures listed in Figure 1), it is included here because of the overall lamellar feature (Figure 1).

*Cylinder-Based Structures.* The overall morphology of the self-assembled structure changes from lamellae to cylinders when the volume of one of its blocks, for example, $f_C$, is increased or decreased. The basic structure of the ordered phases in this case will be *AB* cylinders in a matrix composed of the majority *C* blocks or *C* cylinders in a matrix composed of the majority *AB* blocks. The repulsion between the *A* and *B* blocks leads to separation of these two blocks, resulting in various cylinder-based ordered phase of the system. As shown in Figure 2, the different separation patterns of the *AB* blocks within the cylinders, as well as the possibility of differently oriented *AB*-cylinders, leads to the formation of various hierarchically ordered phases.

The two basic patterns of *AB* separation within a cylinder are the concentric rings (parallel layers) or alternative disks (perpendicular layers). A combination of these two basic *AB* patterns and the arrangement of the cylinders results in the formation of a number of hierarchically structured phases, including square cylinders (SCylParallel, SCylPendicular) and hexagonal cylinders (HCylParallel, HCylPendicular), as shown in Figure 2. It is interesting to notice that the hierarchically ordered cylindrical phases have been observed in the experiments of Matsushita et al.[32]

One possible arrangement of the *AB* cylinders is for them to orient at different directions. Examples of these exotic ordering patterns are the alternative cylinders (ACn), where n = 2, 3, and 4. Specifically, the AC2 has layers of parallel cylinders oriented perpendicularly to each other (Figure 2), the AC3 has cylinders oriented perpendicularly to each other along three different directions, whereas the AC4 has cylinders oriented along four different directions (along four diagonal lines of a cube). Another representation of the AC4 structure is obtained by using the SCFT solution to produce a density plot, as shown in Figure 2.

Finally, when the volume fraction of the *C* blocks is smaller than 0.5, the block copolymers can form *C* cylinders in the *AB* matrix. For block copolymers with immiscible *AB* blocks, *AB* separation occurs in the matrix, leading to the formation of two additional cylinder-based structures (SCyl2 and HCyl2), as shown in Figure 2.

*Sphere- and Gyroid-Based Structures.* Similar to the case of diblock copolymers, order−order transitions from lamellae to gyroid, cylinders, and spheres can be induced by increasing the volume fraction of the *C* blocks, $f_C$. The separation of the *A* and *B* blocks within the domains can then lead to ordered phases with overall structures dictated by the diblock copolymer phases. In particular, ordered phases based on spheres and gyroids are obtained, as shown in Figures 3 and 4.

The separation pattern of the *A* and *B* blocks within spherical domains is dominated by the simple core−shell structures, as shown in Figure 3. Different arrangement of the spheres leads to different ordered phases. In addition to the well-known BCC and FCC structures, we have obtained the A15 and S+ phases as metastable solutions of the *ABC* triblock star copolymers. It is interesting to notice that the A15 and S+ structure has two and four additional spheres on the face of the cubic unit cell of a BCC structure, respectively (Figure 3).

The basic structure of the gyroids is the *AB* cylinders. The separation of the *A* and *B* blocks within the cylinders follows the parallel (core−shell) or perpendicular (segmented) patterns. The combination of the *AB* separation pattern and gyroid structure leads to the formation of a number of gyroid-based structures, including core−shell single gyroids (CS-SGyroid), core−shell double-gyroids (CS-DGyroid), seg-
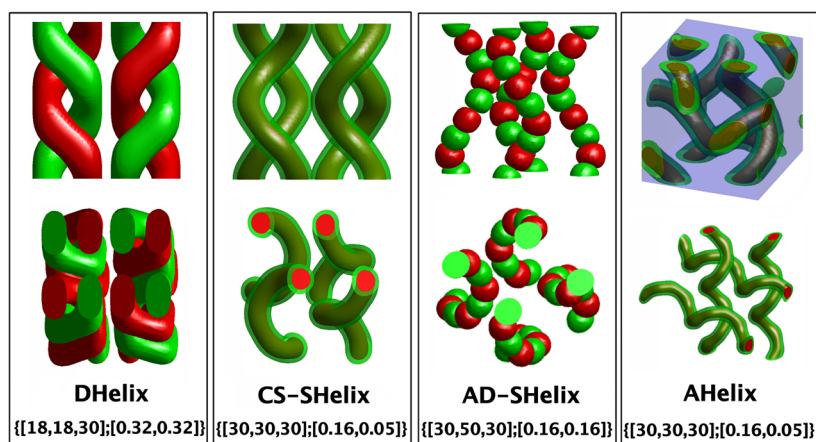
**Figure 5.** Typical helix phases captured in our simulation. Double helix (DHelix), single helix (SHelix), and hierarchical single helix (HierHelix) are quadratically pacted. As for alternative helix (AHelix), it is similar to SHelix to some extent but with two different orientation. All figures here are plotted in cubic, except the bottom illustration of AHelix, which is reconstructed from Fourier coefficients in the well-selected region for a clear illustration of the whole structure.
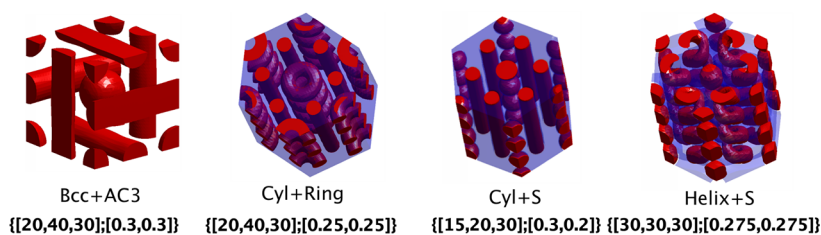


**Figure 6.** Mixed structures captured in our simulation. The possibility of combination among basic structures like spheres, cylinder, rings, and helices are clearly demonstrated by these Figures.
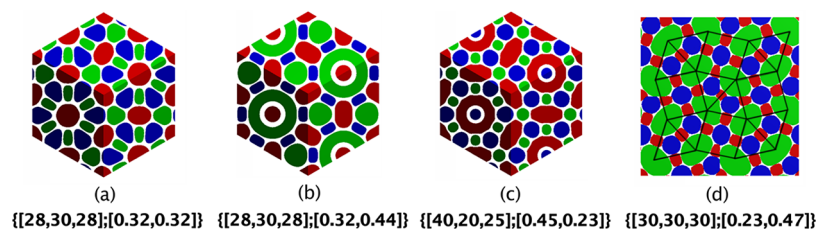


**Figure 7.** Selected 2D structures captured in our simulation.

mented single gyroids (AS-SGyroid), and segmented double gyroids (AS-DGyroid) (Figure 4).

*Helix-Based Structures.* Most of the structures described above can be derived from the ordered phases of diblock copolymers. There are, however, many other phases that do not have their diblock copolymer counterparts. One of these exotic structures is the various helix structures found in triblock copolymer melts[19,42] and diblock copolymers under confinement.[43] For the case of cylinder-forming block copolymers, the formation of helices is due to soft or hard confinement of these cylinders. For the *ABC* star triblock copolymers considered here, the basic structure is composed of *AB*-cylinders embedded in the *C* matrix. Under appropriate conditions, these *AB* cylinders tend to form helices due to spatial constraints. Furthermore, the *A* and *B* within the cylinders can separate into core−shell or segmented patterns. Combinations of these variations lead to a number of different ordered helix phases shown in Figure 5. It should be pointed out that the helices formed by the *ABC* star triblock copolymers are also clearly different from those recently obtained in *ABC* linear copolymers.[19,42]

*Combination of Basic Structures.* Besides the various structures involving helices, another class of possible candidate structures can be generated by combining different structural elements. Applying this strategy to the *ABC* star triblock copolymers leads to a number of novel ordered phases, which are combinations of different structural elements, such as spheres, cylinders, rings, and helices composed of *A* blocks in a matrix of the majority *BC* blocks (Figure 6).

One example of these novel structures is formed by combining the alternative cylinders AC3 and BCC, leading to a composed ordered phase labeled as the BCC+AC3 in Figure 6. Another example is provided by combining parallel cylinders with hexagonally packed stacks of rings or spheres, forming the Cyl+Ring and Cyl+S phases shown in Figure 6. From our calculations, we also observe the twisting of parallel cylinders in the Cyl+S phase, ultimately forming a combination of helices and spheres (Helix+S). It should be pointed out that all of these novel order structures are solutions of the SCFT equations, and thus they are metastable phases of the system.

*Two-Dimensional Tiling Patterns.* One class of structures unique to the *ABC* star triblock copolymers is the 2D tiling
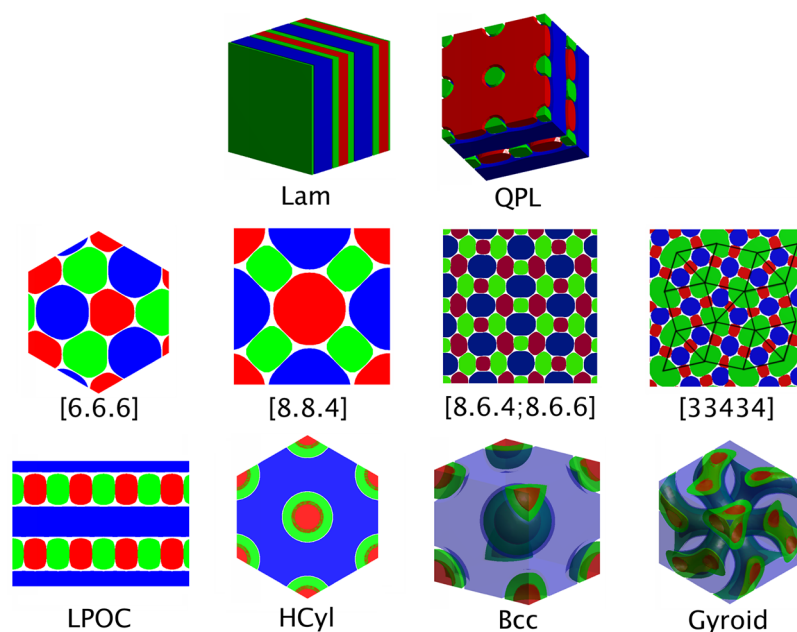
**Figure 8.** Stable phases, according to our 3D simulations, in the phase diagram with fixed Flory−Huggins interaction parameters $\chi_{BC}N = \chi_{AC}N = \chi_{AB}N = 30$. Monomers A, B, and C are denoted by red, green, and blue colors.

patterns observed in previous experiments, MC simulations, and SCFT calculations.[30,38] This class of structures is basically cylindrical in nature, with different cross sections of the blocks assuming different shapes. Some of the 2D tiling patterns obtained from our SCFT calculations are shown in Figure 7. Many of these structures, such as Figure 7a,d, have been obtained in previous experiments by Hayashida et al.,[30] as well as in SCFT calculations by Li et al.[38] It is also interesting to point out that the structure shown in Figure 7d (also known as $3^2434$ in the literature), is closely related to the 12-fold quasi-crystal observed in ABC star triblock copolymers.[44]

**Phase Diagram of Symmetrically Interacting ABC Star Triblock Copolymers.** In this section, we present a phase diagram of symmetrically interacting ABC star triblock copolymers with fixed Flory−Huggins parameters, $\chi = [\chi_{BC}, \chi_{AC}, \chi_{AB}] = [30, 30, 30]$. This specific system is chosen due to numerous previous studies of the same model system so that the power of the proposed strategy of discovering ordered phases can be compared with previous results. It is worth pointing out that most previous experimental and theoretical studies of ABC star triblock copolymer focus on the 2D tiling patterns. In particular, a detailed phase diagram containing a large number of tiling patterns has been constructed for ABC star triblock copolymers with $\chi = [30, 30, 30]$ by Zhang et al. using a generic spectral method to solve the SCFT equations.[39] They conclude that tiling patterns including [6.6.6], [8.8.4], [12.6.4], [8.6.4;8.6.6], [10.6.4;10.6.4;10.6.6], and [8.6.4;8.8.4;12.6.4;12.8.4] are stable phases according to their 2D simulation.

We have carried out a large number of SCFT calculations for the symmetrically interacting ABC star triblock copolymers with $\chi = [30, 30, 30]$. The calculations result in a large number of candidate phases including 2D tiling patterns and various 3-D ordered phases. It is interesting to notice that the tiling pattern [8.6.4;8.8.4;12.6.4;12.8.4] obtained by Zhang et al. was not obtained in our 3D simulation. All other tiling patterns presented by Zhang et al. have been obtained in our SCFT calculations. It should be pointed out that the tiling pattern

[8.6.4;8.8.4;12.6.4;12.8.4] occupies a small region where 3D structures are found to be stable phases in the current study. These SCFT calculations provide an array of candidate structures, including all 3D ordered phases presented above and the 2D tiling patterns obtained in our calculations. These ordered phases are used to construct phase diagram of the system. It is not surprising that many of the candidate structures are only metastable phases of the system. For example, the tiling patterns such as [12.6.4], [10.6.4;10.6.4;10.6.6], and [8.6.4;8.8.4;12.6.4;12.8.4], which are stable in the 2D calculations,[39] become metastable phases. For the symmetrically interacting ABC star triblock copolymers, the number of stable phases is drastically reduced and all of the stable structures are shown (Figure 8).

Because of the symmetry of the phase diagram, we only need to consider 1/6 of the phase triangle. Furthermore, we focus on five typical lines connecting the center ($f_A = f_B = f_C = 1/3$) of the phase diagram to the AB diblock copolymer side ($f_C = 0$) located at $f_A = [0.00, 0.17, 0.22, 0.33, 0.5]$, corresponding to disordered (D), sphere (S), cylinder (C), gyroid (G), and lamellae (L) phases (Figure 9). At the center of the phase diagram, the stable phase is the 2D tiling pattern [6, 6, 6]. Phase-transition sequences from this tiling pattern to the different diblock copolymer phases (D, S, C, G, and L) are predicted by our SCFT calculations.

The predicted order−order phase transition sequences along the five paths in the phase diagram are shown in Figure 9. It is interesting to notice that although the transition sequences are all different the transitions exhibit a general trend in that the overall morphology follows the sequence of spheres to cylinders to gyroid to lamellae and finally to the tiling patterns. This trend of overall morphologies is clearly shown for the case of Line II (Figure 9) connecting the center of the phase diagram to the BCC phases at $f_A = 0.17$.

Finally, it should be pointed out that the phase diagram obtained in the current SCFT calculations is consistent with the 2D SCFT calculations carried out by Zhang et al.[39] near the center of the phase triangle (dominated by tiling patterns).
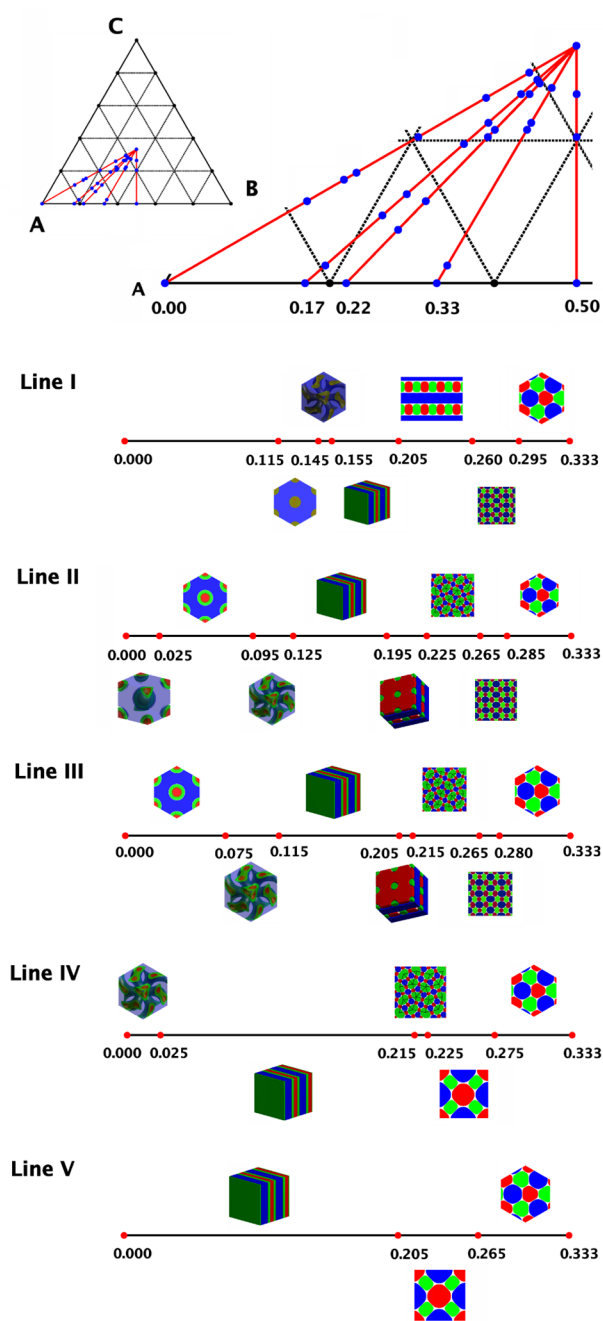
**Figure 9.** Phase diagram with equally fixed Flory–Huggins interaction parameters $\chi_{BC}N = \chi_{AC}N = \chi_{AB}N = 30$ and phase transition sequence along five typical lines, where monomer fraction $f_A$ starts with $f_{A0} =$ [0.00, 0.17, 0.22, 0.33, 0.5], respectively (equivalently connecting the typical diblock phases like disorder, sphere, cylinder, gyroid, and lamellae to the triangle center, where it is dominated by tiling pattern [6.6.6]). Subfigures (lines I–V) illustrate the phase-transition sequence, where the numbers under these lines denote the value of the monomer fraction $f_B$ at the point of phase boundaries.

Furthermore, the predicted phase diagram is consistent with available experimental results.[27–34]

## ■ CONCLUSIONS AND DISCUSSION

In this work, we have developed a strategy to discover ordered phases of block copolymers within the framework of the SCFT and applied the proposed strategy to *ABC* star triblock copolymers. A two-step strategy is proposed to explore the phase behavior of multiblock copolymers. The first step involves an efficient method to obtain as many solutions of the SCFT equations as possible. This is achieved by a combination of fast numerical algorithm and various initialization schemes, leading to a library of candidate structures. In the second step, these candidates structures are used as input to more accurate methods to compute their free energies, which are used to construct phase diagrams of the system. The power of the proposed strategy is demonstrated by applying it to the phase behavior of *ABC* star triblock copolymers. A large number of previously unknown candidate phases for the system has been obtained. All of these complex ordered phases are solutions of the SCFT equations; therefore, they correspond to metastable phases of the system.

To generate more candidate structures, we have found that it is fruitful to extend the initialization schemes beyond random initialization. We have generated initial configurations using (1) knowledge from previous experiments and theories; (2) knowledge from related systems, for example, diblock copolymers; (3) combination and interpolation of known structures; and (4) random initial configurations. Using these diverse strategies of initialization, a great number of candidate ordered phases have been obtained as solutions of the SCFT equations. The availability of these candidate phases enables the construction of phase diagrams for block copolymer systems.

The phase behavior of *ABC* star triblock copolymers has been examined using the proposed strategy. Our extensive SCFT calculations with various initial configurations reveal a large number of solutions of the SCFT equations, which are stable and metastable ordered phases of the system. These complex ordered phases can be usefully categorized by their overall morphologies. In particular, it is observed that the candidate structures can be classified into lamellae based structures, cylinder-based structures, sphere- and gyroid-based structures, helix-based structures, and a combination of basic structures. The occurrence of these complex ordered phases can be attributed to the fact that in *ABC* star triblock copolymers, the junction points are confined to 1-D curves by the topology of the copolymers.[24,25] These candidate phases can be used as input to construct phase diagrams of *ABC* star triblock copolymers. In particular, a phase diagram for the symmetrically interacting *ABC* triblock copolymers has been obtained, revealing a number of interesting three-dimensionally ordered phases.

It should be emphasized that using different initial configurations for the iteration procedure to solve the SCFT equations is crucial to obtain different solutions of the SCFT equations. A common practice in the literature is to use random initial configurations generated in real- or reciprocal-space, as proposed by Drolet and Fredrickson.[20] This approach assumes that the phase obtained for a given set of parameters is generally the stable one or the phase with the lowest free energy. This strategy does reproduce the correct stable phase for simple systems, such as the lamellae or cylinders of diblock copolymers. However, utilizing random initial fields alone may leave many potential morphologies unexplored. To examine the capability of the random initialization method, we have carried out a large number of calculations using random fields generated in real and reciprocal spaces. Specifically for the case with $\chi_{AB} = 30$, $\chi_{AC} = \chi_{BC} = 40$, and $f_A = f_B = 0.2$, we have carried out 1044 calculations with random initial fields in real space and 1044 calculations with random initial fields in reciprocal space. We obtained similar results for initial fields in

real and reciprocal space. Among the 2088 simulations, 203 of them did not converge and 182 of them led to the disordered phase. The majority (1268) of the 2088 simulations resulted in the LPOC structure, which is the phase with the lowest free energy ($f = 0.003066$). The second major phase from this set of simulations was the LZZ ($f = 0.00542$), which occurred 421 times. Finally, the LAOC structure, whose free energy ($f = 0.003068$) is almost generate with the LPOC phase, was observed 14 times. The other metastable ordered phases (LHR, HPL, and Lam) with much higher free energy, which could be generated using special initializations, were not observed in these 2088 simulations. Although these calculations were only carried out for one set of parameters, they explicitly illustrate the point that using random initialization alone can generate a number of ordered stable phases, but it may miss many potential candidate structures.

## ■ AUTHOR INFORMATION

### Corresponding Author
*E-mail: pzhang@pku.edu.cn (P.Z.); shi@mcmaster.ca (A.-C.S.).

### Notes
The authors declare no competing financial interest.

## ■ ACKNOWLEDGMENTS

## ■ REFERENCES

(1) Hamley, I. W. *Developments in Block Copolymer Science and Technology*; Wiley: New York, 2004.
(2) Abetz, V.; Simon, P. F. W. *Adv. Polym. Sci.* **2005**, *189*, 125−212.
(3) Park, C.; Yoon, J.; Thomas, E. L. *Polymer* **2003**, *44*, 6725.
(4) Matsen, M. W. *Eur. Phys. J. E.* **2009**, *30*, 361.
(5) Bates, F. S.; Hillmyer, M. A.; Lodge, T. P; Bates, C. M.; Delaney, K. T.; Fredrickson, G. H. *Science* **2012**, *336*, 434.
(6) Meuler, A. J.; Hillmyer, M. A.; Bates, F. S. *Macromolecules* **2009**, *42*, 7221−7250.
(7) Matsen, M. W. *J. Phys.: Condens. Matter* **2002**, *14*, R21.
(8) Fredrickson, G. H. *The Equilibrium Theory of Inhomogeneous Polymers*; Oxford University Press: New York, 2006.
(9) Helfand, E.; Wasserman, Z. R. *Macromolecules* **1976**, *9*, 879.
(10) Shull, K. R. *Macromolecules* **1992**, *25*, 2122.
(11) Vavasour, J.; Whitmore, M. *Macromolecules* **1992**, *25*, 5477.
(12) Matsen, M. W.; Schick, M. *Phys. Rev. Lett.* **1994**, *72*, 2660.
(13) Matsen, M. W. *J. Chem. Phys.* **1997**, *108*, 785.
(14) Matsen, M. W. *Macromolecules* **1995**, *28*, 5765.
(15) Matsen, M. W.; Bates, F. S. *Macromolecules* **1996**, *29*, 1091.
(16) Matsen, M. W. *Macromolecules* **2012**, *45*, 2161.
(17) Tyler, C. A.; Morse, D. C. *Phys. Rev. Lett.* **2005**, *94*, 208302.
(18) Tyler, C. A.; Qin, J.; Bates, F. S.; Morse, D. C. *Macromolecules* **2007**, *40*, 4654−4668.
(19) Guo, Z. J.; Zhang, G. J.; Qiu, F.; Zhang, H. D.; Yang, Y. L.; Shi, A. C. *Phys. Rev. Lett.* **2008**, *101*, 028301.
(20) Drolet, F.; Fredrickson, G. H. *Phys. Rev. Lett.* **1999**, *83*, 4317−4320.
(21) Bohbot-Raviv, Y.; Wang, Z. G. *Phys. Rev. Lett.* **2000**, *85*, 3428−3431.
(22) Tzeremes, G.; Rasmussen, K.; Lookman, T.; Saxena, A. *Phys. Rev. E* **2002**, *65*, 041806.
(23) Cochran, E. W.; Garcia-Cervera, C. J.; Fredrickson, G. H. *Macromolecules* **2006**, *39*, 2449−2451.
(24) Okamoto, S.; Hasegawa, H.; Hashimoto, T.; Fujimoto, T.; Zhang, H.; Kazama, T.; Takano, A.; Isono, Y. *Polymer* **1997**, *38*, 5275−5281.
(25) Sioula, S.; Hadjichristidis, N.; Thomas, E. L. *Macromolecules* **1998**, *31*, 8429−8432.
(26) Hückstädt, H.; Göpfert, A.; Abetz, V. *Macromol. Chem. Phys.* **2000**, *201*, 296−307.
(27) Takano, A.; Wada, S.; Sato, S.; Araki, T.; Hirahara, K.; Kazama, T.; Kawahara, S.; Isono, Y.; Ohno, A.; Tanaka, N.; Matsushita, Y. *Macromolecules* **2004**, *37*, 9941−9946.
(28) Takano, A.; Kawashima, W.; Noro, A.; Isono, Y.; Tanaka, N.; Dotera, T.; Matsushita, Y. *J. Polym. Sci., Part B: Polym. Phys.* **2005**, *43*, 2427−2432.
(29) Hayashida, K.; Kawashima, W.; Takano, A.; Shinohara, Y.; Amemiya, Y.; Nozue, Y.; Matsushita, Y. *Macromolecules* **2006**, *39*, 4869−4872.
(30) Hayashida, K.; Takano, A.; Arai, S.; Shinohara, Y.; Amemiya, Y.; Matsushita, Y. *Macromolecules* **2006**, *39*, 9402−9408.
(31) Matsushita, Y. *Macromolecules* **2007**, *40*, 771−776.
(32) Hayashida, K.; Saito, N.; Arai, S.; Takano, A.; Tanaka, N.; Matsushita, Y. *Macromolecules* **2007**, *40*, 3695−3699.
(33) Matsushita, Y.; Takano, A.; Hayashida, K.; Asari, T.; Noro, A. *Polymer* **2009**, *50*, 2191−2203.
(34) Matsushita, Y.; Hayashida, K.; Takano, A. *Macromol. Rapid Commun.* **2010**, *31*, 1579−1587.
(35) Gemma, T.; Hatano, A.; Dotera, T. *Macromolecules* **2002**, *35*, 3225−3237.
(36) Huang, C. I.; Fang, H. K.; Lin, C. H. *Phys. Rev. E* **2008**, *77*, 031804.
(37) Tang, P.; Qiu, F.; Zhang, H. D.; Yang, Y. L. *J. Phys. Chem. B* **2004**, *108*, 8434−8438.
(38) Li, W. H.; Xu, Y. C.; Zhang, G. J.; Qiu, F.; Yang, Y. L.; Shi, A. C. *J. Chem. Phys.* **2010**, *133*, 064904.
(39) Zhang, G. J.; Qiu, F.; Zhang, H. D.; Yang, Y. L.; Shi, A. C. *Macromolecules* **2010**, *43*, 2981−2989.
(40) Xu, Y.; Li, W.; Qiu, F.; Zhang, H.; Yang, Y.; Shi, A.-C. *J. Polym. Sci., Part B* **2010**, *48*, 1101−1109.
(41) Shi, A. C. *Developments in Block Copolymer Science and Technology*; Wiley: New York, 2004.
(42) Li, W. H.; Qiu, F.; Shi, A. C. *Macromolecules* **2012**, *45*, 503−509.
(43) Yu, B.; Sun, P. C.; Chen, T. H.; Jin, Q. H.; Ding, D. T.; Li, B. H.; Shi, A. C. *Phys. Rev. Lett.* **2006**, *96*, 138306.
(44) Hayashida, K.; Dotera, T.; Takano, A.; Matsushita, Y. *Phys. Rev. Lett.* **2007**, *98*, 195502.
(45) Grason, G. M.; Kamien, R. D. *Macromolecules* **2004**, *37*, 7371.
(46) Milner, S. T. *Macromolecules* **1994**, *27*, 2333.